Direct Measurements of an Increased Threshold for Stimulated Brillouin Scattering with Polarization Smoothing in Ignition Hohlraum Plasmas

D. H. Froula,* L. Divol, R. L. Berger, R. A. London, N. B. Meezan, D. J. Strozzi, P. Neumayer, J. S. Ross, S. Stagnitto,+ L. J. Suter, and S. H. Glenzer

L-399, Lawrence Livermore National Laboratory, P.O. Box 808, Livermore, California 94551, USA

(Received 13 November 2007; published 10 September 2008)

We demonstrate a significant reduction of stimulated Brillouin scattering by polarization smoothing in large-scale high-temperature hohlraum plasma conditions where filamentation is measured to be negligible. The stimulated Brillouin scattering experimental threshold (defined as the intensity at which 5% of the incident light is backscattered) is measured to increase by a factor of 1.7 ± 0.2 when polarization smoothing is applied. An analytical model relevant to inertial confinement fusion plasma conditions shows that the measured reduction in backscatter with polarization smoothing results from the random spatial variation in polarization of the laser beam, not from the reduction in beam contrast.

DOI: 10.1103/PhysRevLett.101.115002 PACS numbers: 52.38.Bv, 52.25.Os, 52.35.Fp, 52.50.Jm

Inertial confinement fusion (ICF) at megajoule laser facilities [1,2] requires a high degree of uniformity in the laser focal spot intensity, for the direct drive approach [3], and efficient laser beam propagation, for the indirect-drive approach [4]. The current indirect-drive designs rely on laser-smoothing techniques to enhance laser beam propagation through centimeter-long, low-density ($n_e \simeq 5 \times 10^{20}$ cm^{-3}), high-temperature ($T_e > 2$ keV) plasmas which allows the laser energy to be efficiently converted into soft x rays in the hohlraum wall. Previously, polarization smoothing has been shown to reduce backscatter through the mitigation of filamentation [5–8], but for conditions where there is no filamentation, as expected in ICF, no experiment to date has quantified the effect of polarization smoothing on backscatter [9–12].

In this study, we present the first experiments that quantify the reduction of stimulated Brillouin scattering (SBS) by polarization smoothing in a high-temperature ($T_e \simeq 3$ keV) ICF relevant plasma where filamentation effects are measured to be negligible. Figure 1 shows that the SBS reflected power is lower at all times when polarization smoothing is applied. The SBS intensity threshold is measured to increase by a factor of 1.7 ± 0.2 where the threshold for backscatter is defined as the intensity (I_{th}) at which 5% of the incident power is backscattered. An analytical model is presented that explains the effect of beam smoothing on the backscatter threshold which results from the mixing of the polarizations, not a reduction of the beam contrast.

A hohlraum target platform for studying laser-plasma interactions in 2-mm long high-temperature plasmas has been developed by aligning an interaction beam down the axis of a gas-filled gold cylinder (hohlraum); this allows direct measurements of the laser beam propagation and transmission at ignition hohlraum plasma conditions [13]. The hohlraum is heated by 33, 1-ns square pulsed, frequency tripled ($\lambda_0 = 351$ nm) laser beams (14.5 kJ) at the OMEGA Laser Facility [14]. The heater beams are smoothed by elliptical phase plates that project a $\sim$250 μm diameter intensity spot at the 800 μm diameter laser entrance holes.

The 1.6-mm diameter, 2-mm long hohlraum targets are filled with 1 atm of a 30% CH_4 and 70% C_3H_8 gas mix. The uniform plasma conditions along the interaction beam path ($T_e \simeq 3$ keV, $n_e \simeq 5 \times 10^{20}$ cm^{-3}) are comparable to the plasma conditions that the inner beam propagates through on current targets planned for ignition experiments on the National Ignition Facility [15]. These plasma conditions have been validated using Thomson scattering [13] and by two-dimensional HYDRA [16] hydrodynamic simulations.

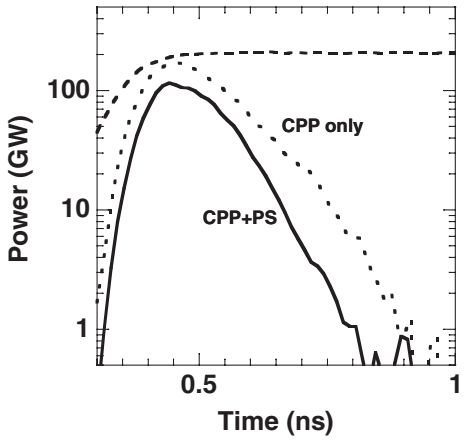

FIG. 1. The measured SBS power is shown to be lower at all times when polarization smoothing (solid curve) is added to a CPP-smoothed beam (dotted curve); an incident power of 200 GW is used (dashed curve). The reflectivity peaks early in time as the interaction beam reaches maximum power and the plasma is cold ($T_e \sim 2$ keV); the backscatter decreases rapidly as the electron temperature increases [26].

Figures 2(a) and 2(b) show the simulated laser spots at best focus for the 3ω interaction beam focused by a $f/6.7$ lens. The simulated spot is generated using the OMEGA aberration model [17] and the measured near-field phase of the continuous phase plate (CPP) [18]. The average on axis intensity at best focus for this beam is $I = 1.05 \times P$ (in GW) $\times 10^{13}$ W cm^{-2}, where P is the incident laser beam power ranging from 50 to 500 GW.

A new birefringent polarization smoothing (PS) crystal has been designed for these experiments that sufficiently separates the speckles in the far field without affecting the average spot size. After the laser beam propagates through this crystal, two beams separated by a small angle are created with equal intensity and orthogonal polarizations. The separation between the two beams was characterized to be 15 μm at best vacuum focus [Fig. 2(c)]. When used with a CPP, this 15 μm separation at the focal plane is sufficient to decorrelate the two speckle patterns while having a minimal effect on the average intensity of the laser beam [Fig. 2(d)].

Light scattered from the interaction beam is measured using a full-aperture backscatter station (FABS) [19], a near backscatter imager (NBI) [20], and a 3ω transmitted beam diagnostic (3ωTBD) [21]. Light scattered back into the original beam cone is collected by the FABS. The NBI measures backscattered light outside the original beam cone that reflects from a plate surrounding the interaction beam. A new calibration technique was employed using a pulsed calibration system to deliver a known energy to the NBI scatter plate and the FABS calorimeters. The resulting uncertainty in the measurements of the total SBS energy is 5%. The 3ωTBD allows us to measure the interaction beam power and a near-field image after propagation through the plasma, within twice the original $f/6.7$ beam cone.

Figure 3 is the main experimental result of this Letter. It shows that the SBS intensity threshold for the CPP-smoothed laser beam ($I_{\text{th}} = 1.3 \times 10^{15}$ W cm^{-2}) is increased by a factor 1.7 ± 0.2 when polarization smoothing is applied ($I_{\text{th}} = 2.2 \times 10^{15}$ W cm^{-2}). This novel result has been obtained by accessing high electron temperature conditions where filamentation and absorption are mitigated. The SBS power is obtained by averaging the temporally resolved SBS reflectivity over 50 ps, 700 ps after the rise of the heater beams. The error bars are given by the extreme reflectivities within the 50 ps time interval. At 700 ps the plasma has had time to reach an electron temperature of $T_e = 2.7$ keV and the plasma density on axis is still uniform. Late in time the shock wave produced by the ablation of the gold wall reaches the hohlraum axis ($t \simeq 1.1$ ns). Furthermore, our reflectivity measurements have the largest dynamic range around 700 ps; early in time the reflectivities are affected by pump depletion and late in time they are below detection levels (<0.1%).

Figure 3 shows that using 3 Å of smoothing by spectral dispersion (SSD) has no significant effect on SBS. This can be expected in this strongly damped regime where the damping rate of SBS-driven ion acoustic waves $\nu_a \approx 2$ ps^{-1} is much larger than the inverse correlation time introduced by the laser bandwidth. The situation could be quite different in a weakly damped regime, such as in the gold plasma close to the hohlraum wall [22]. Previous observations of SBS reduction through control of filamentation by SSD does not apply to this high electron temperature, moderate intensity experiment, as noted before.

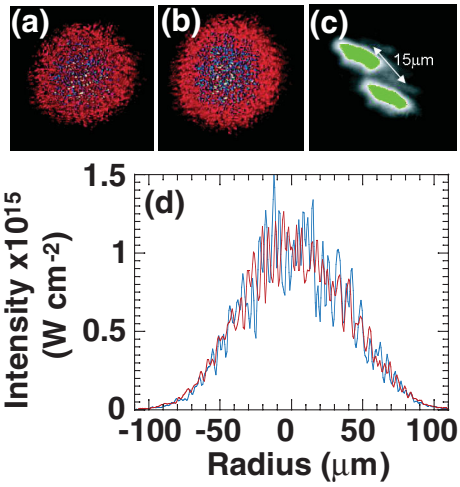

FIG. 2 (color). The far-field intensity distribution is simulated using the OMEGA laser beam aberrations, the (a) measured CPP phase, and the (b) measured PS shift. (c) The polarization shift at the best vacuum focus was measured to be 15 μm. (d) The vacuum transverse intensity profile is compared with (red) and without (blue) polarization smoothing demonstrating that the average intensity of the beam is not modified.

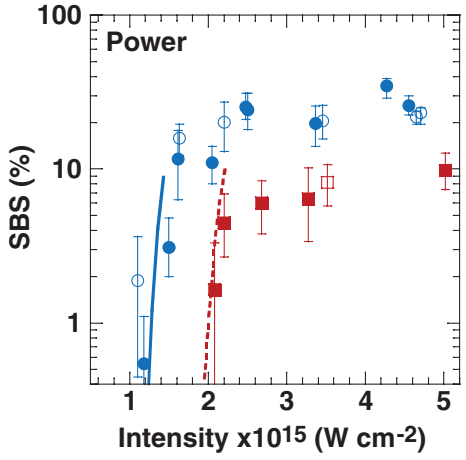

FIG. 3 (color). The measured instantaneous SBS reflectivity at 700 ps is plotted as a function of the average interaction beam intensity; three laser-smoothing conditions are shown: CPP (blue), PS (red), and 3 Å SSD (open symbols). An analytical model that calculates the thresholds is shown for the CPP only (solid blue curve) and when polarization smoothing is applied (dashed red curve).

Figure 4 shows the total energy backscattered and transmitted through the plasma. For low backscatter conditions, more than 75% of the energy is transmitted through the plasma. For an incident laser energy of 200 J, polarization smoothing increases the total energy transmitted from 60% to 70% while the backscattered energy is reduced from 19% to 8%. HYDRA calculates a peak transmission of the interaction beam, excluding backscatter, to be 90% and the time integrated transmission to be 80%.

Figure 5 shows the near-field (lens plane) intensity profile after the interaction beam has propagated through the plasma. No significant difference in beam spray is measured when polarization smoothing is applied; as beam spray is a measure of filamentation, this is direct evidence that filamentation is not the main contribution to the measured effects of polarization smoothing on SBS. Furthermore, less than 5% of the total SBS is measured outside of the FABS for incident interaction beam intensities less than $I < 3 \times 10^{15}$ W cm^{-2}. These results are explained by the fact that the experiments remain below the thermal and ponderomotive filamentation thresholds by interacting with high electron temperature ($T_e \simeq 3$ keV) plasmas and by using moderate laser intensities.

The SBS intensity threshold determined using a detailed 1D model (DEPLETE [23]) predicts the threshold for SBS to be 2×10^{15} W cm^{-2} which is higher than the measured threshold made with a CPP-smoothed laser beam (1.3×10^{15} W cm^{-2}). DEPLETE uses the plasma conditions simulated by HYDRA and the average laser intensity on axis to calculate the laser and backscattered intensities, in steady state, along a 1D ray profile. It solves for the scattered-wave intensity spectrum over a range of frequencies including realistic noise sources and pump depletion.

We have previously shown that three-dimensional whole beam simulations can correctly calculate the SBS threshold by including a realistic description of a CPP-smoothed laser beam [24]. Here we develop an analytical model that explains and quantifies the effect of polarization smoothing without requiring large simulations.

In the strongly damped steady-state regime, the amplification of the backscattered light field A_1 is governed by $\partial_z A_1 = \gamma M_0 A_1$ where $\gamma \approx 8$ mm^{-1} is the strongly damped spatial growth rate for our plasma conditions, at an average intensity of 10^{15} W cm^{-2}. M_0 contains the spatial information about the interaction beam. For a CPP-smoothed beam, $M_0 = |A_0|^2$ is the local intensity normalized to the average. With PS, the fields are separated in two orthogonal polarizations,

$$A_1 = \begin{pmatrix} a_1 \\ a_{1p} \end{pmatrix}$$

and

$$M_0 = \begin{pmatrix} |a_0|^2 & a_0 a_{0p}^* \\ a_0^* a_{0p} & |a_{0p}|^2 \end{pmatrix}.$$

Assuming M_0 constant along the propagation axis z over one correlation length of the laser (i.e., the length of one typical hot spot $L_{sp} = 5f^2\lambda = 78$ μm), one can calculate the amplification factor $\Gamma = |A_1(z + L_{sp})|^2/|A_1(z)|^2$ over a speckle length by exponentiating M_0. The amplification factor for a CPP-smoothed beam, assuming $A_1(z)$ is uncorrelated with M_0, is

$$\Gamma_{CPP} = \langle \exp(G_{sp} I) \rangle_{CPP}, \quad (1)$$

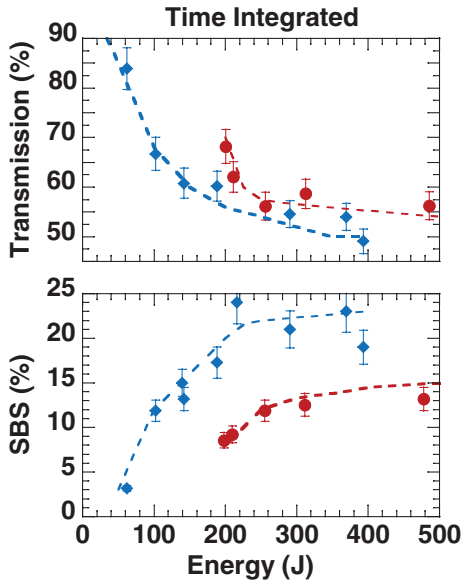

FIG. 4 (color). The time integrated transmission (top) and backscatter (bottom) are plotted as a function of interaction beam energy, with (red circles) and without (blue diamonds) polarization smoothing.

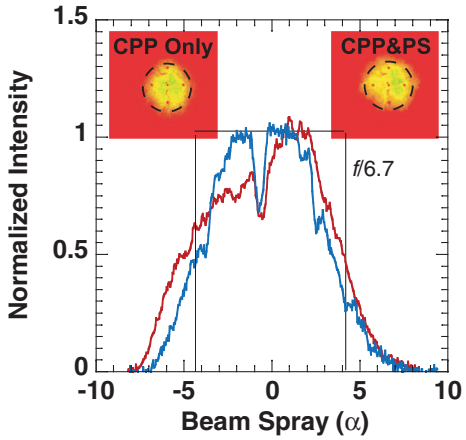

FIG. 5 (color). The intensity profile of the transmitted beam spray is plotted for an incident intensity of 2×10^{15} W cm^{-2} and for two laser beam smoothing conditions: CPP only (blue), and CPP and PS (red). The near-field transmitted beam images are inset. The dashed circles represent a $f/6.7$ cone ($\alpha = 4.3°$) around the center of the beam.

and when polarization smoothing is used, the amplification factor becomes

$$\Gamma_{\mathrm{PS}} = (1 + \langle \exp(G_{\mathrm{sp}} I) \rangle_{\mathrm{PS}})/2, \quad (2)$$

where $\langle\rangle_{\mathrm{CPP}}$ [$\langle\rangle_{\mathrm{PS}}$] means a statical average over the laser intensity distribution, normalized to the average intensity, $p(I) = \exp(-I)$ [$p(I) = 4I\exp(-2I)$]. For a short plasma where the average gain per speckle length is large ($G_{\mathrm{sp}} = 2\gamma L_{\mathrm{sp}} > 1$), the main contribution to the backscatter amplification comes from the most intense speckles [25] which is eventually enhanced by self-focusing; polarization smoothing has been shown to reduce the laser power in these intense speckles, thereby mitigating backscatter [5–7].

This experiment, and most ICF relevant conditions, are in a very different regime; the amplification occurs over many speckles ($L \gg L_{\mathrm{sp}}$), where L is the plasma length ($L \approx 19 L_{\mathrm{sp}}$ for this experiment), and the gain per speckle is small ($G_{\mathrm{sp}} < 1$). The overall amplification is then $\Gamma^{L/L_{\mathrm{sp}}} \gg 1$. In this case, the amplification term in Γ can be expressed as $\langle \exp(G_{\mathrm{sp}} I) \rangle_{\mathrm{PS}} = (1 - G_{\mathrm{sp}}/2)^{-2}$ when polarization smoothing is applied and $\langle \exp(G_{\mathrm{sp}} I) \rangle_{\mathrm{CPP}} = (1 - G_{\mathrm{sp}})^{-1}$ when it is not. To first order in G_{sp}, these terms are equal and the reduction in beam contrast with polarization smoothing does not affect the backscatter. The strong increase in the SBS threshold with polarization smoothing is then due to the factor $1/2$ in the amplification factor (Γ_{PS}) which comes from the fact that on average only one of the polarizations is amplified over a speckle length (L_{sp}) at a given transverse location.

For long plasmas and moderate gain per speckle, it is the short correlation length of the interaction beam polarization, not the reduction in beam contrast, that explains the effect of polarization smoothing on SBS. The overall increase α in the SBS threshold when applying polarization smoothing is calculated by setting $\Gamma_{\mathrm{PS}}(\alpha G_{\mathrm{sp}}) = \Gamma_{\mathrm{CPP}}(G_{\mathrm{sp}})$; for $G_{\mathrm{sp}} < 1$ one finds

$$\alpha = 2 - \frac{G_{\mathrm{sp}}}{2} \frac{1 - G_{\mathrm{sp}}/2}{1 - G_{\mathrm{sp}}/4}. \quad (3)$$

For the conditions of Fig. 3 and the measured threshold intensity of $I_{\mathrm{th}}^{\mathrm{CPP}} = 1.3 \times 10^{15}\ \mathrm{W\,cm^{-2}}$, the 1D gain is $G_{\mathrm{1D}} = 13.8$. This leads to a gain per speckle of $G_{\mathrm{sp}} = 0.7$ and, according to Eq. (3), an increase in threshold of $\alpha = 1.72$ when polarization smoothing is applied, which is consistent with the measurements.

In summary, we have experimentally demonstrated that using polarization smoothing increases the intensity threshold for stimulated Brillouin scattering by a factor 1.7 ± 0.2 in large-scale high-temperature hohlraum plasma conditions. An analytical model explains that this effect is primarily due to the random polarization of the laser beam, not its lower contrast, and predicts an increase in the threshold between $5/3$ and 2 for ICF conditions, which is consistent with the experimental results. This study validates polarization smoothing as a key beam conditioning option for future ICF facilities. Its implementation on the National Ignition Facility will allow the use of smaller focal spots (i.e., higher laser intensities), leading to higher radiation temperatures in hohlraums and more symmetry tuning flexibility for ignition attempts.

This work was supported by LDRD 06-ERD-056 and performed under the auspices of the U.S. Department of Energy by Lawrence Livermore National Laboratory under Contract No. DE-AC52-07NA27344.

*froula1@llnl.gov

[+]Current address: Laboratory for Laser Energetics, Rochester, NY, USA.

[1] E. Moses *et al.*, Fusion Sci. Technol. **47**, 314 (2005).
[2] C. Cavailler, Plasma Phys. Controlled Fusion **47**, B389 (2005).
[3] T. R. Boehly *et al.*, J. Appl. Phys. **85**, 3444 (1999).
[4] J. D. Lindl *et al.*, Phys. Plasmas **11**, 339 (2004).
[5] J. Fuchs *et al.*, Phys. Rev. Lett. **84**, 3089 (2000).
[6] S. Huller *et al.*, Phys. Plasmas **5**, 3794 (1998).
[7] R. Berger *et al.*, Phys. Plasmas **6**, 1043 (1999).
[8] S. H. Glenzer *et al.*, Nature Phys. **3**, 716 (2007).
[9] B. Macgowan *et al.*, Phys. Plasmas **3**, 2029 (1996).
[10] D. S. Montgomery *et al.*, Phys. Plasmas **3**, 1728 (1996).
[11] S. H. Glenzer *et al.*, Phys. Plasmas **8**, 1692 (2001).
[12] J. D. Moody *et al.*, Phys. Rev. Lett. **86**, 2810 (2001).
[13] D. Froula *et al.*, Phys. Plasmas **13**, 052704 (2006).
[14] T. Boehly *et al.*, Opt. Commun. **133**, 495 (1997).
[15] D. A. Callahan *et al.*, Phys. Plasmas **13**, 056307 (2006).
[16] M. M. Marinak *et al.*, Phys. Plasmas **8**, 2275 (2001).
[17] T. Kessler, Laboratory For Laser Energetics Review, Technical Report No. 31, 1987.
[18] S. Dixit *et al.*, Opt. Lett. **21**, 1715 (1996).
[19] S. P. Regan *et al.*, Phys. Plasmas **6**, 2072 (1999).
[20] P. Neumayer *et al.*, Rev. Sci. Instrum. (to be published).
[21] D. H. Froula *et al.*, Rev. Sci. Instrum. **77**, 10E507 (2006).
[22] L. Divol, Phys. Rev. Lett. **99**, 155003 (2007).
[23] D. J. Strozzi *et al.*, Phys. Plasmas (to be published).
[24] D. H. Froula *et al.*, Phys. Rev. Lett. **100**, 015002 (2008).
[25] H. A. Rose and D. F. Dubois, Phys. Rev. Lett. **72**, 2883 (1994).
[26] D. H. Froula *et al.*, Phys. Rev. Lett. **98**, 085001 (2007).